# Dynamic analysis of human walking

François Faure, Gilles Debunne, Marie-Paule Cani, Franck Multon

# Dynamic analysis of human walking

François Faure, Gilles Debunne,
Marie-Paule Cani-Gascuel, Franck Multon ‡

iMAGIS[†]-GRAVIR / IMAG
BP 53, F-38041 Grenoble cedex 09, France
Francois.Faure@imag.fr, Gilles.Debunne@imag.fr, Marie-Paule.Gascuel@imag.fr
‡ IRISA
Campus de Beaulieu, 35042 Rennes Cedex, France
Franck.Multon@irisa.fr

Definitive version - Off print

**Abstract**

Synthetising realistic animations of human figures should benefit from both a priori biomechanical knowledge on human motion and physically-based simulation techniques, eager to adapt motion to the specific environment in which it takes place. This paper performs a first step towards this goal, by computing and analyzing the internal actuator forces involved when the human figure performs specific walk motions. The computations rely on a robust simulator where forward and inverse dynamics are combined with automatic collision detection and response. The force curves we obtain give interesting information on the respective action of muscles in various styles of walks. Our further plans include parameterizing them and using them to control physically-based simulations of walk motions.

## 1 Introduction

Two main approaches have been used for generating walking motions in Computer Animation. The first one is to capture or to create several human motions and to deform or combine them in order to generate and control a large variety of virtual motions [BC93, UAT95, BW95, WP95]. However, these methods can only generate walking on a flat ground, without obstacles. The second one is to compute a physically-based simulation of the motion [BC89]. The body of the human figure is provided with actuators at hinges, which represent simplified versions of muscles [HWBO95, LvdP96]. A controller computes the actuators actions over time, and the resulting motion is integrated according to the interactions with the virtual environment. Although such controllers could be generated from random search and optimization [NM93, vdPF93, RGBC96, LvdPF96], exploiting biomechanical knowledge on human walking seems a better approach [HWBO95]. However, this requires much skill since biomechanics analyses the kinematics of captured motion while simulators take the internal actuator forces as an entry.

In this paper, we compute and analyse the actuator forces needed for a human figure to perform different walking gaits. We first convert a priori kinematic knowledge on human walking described by biomechanics into parametrized automatons delivering angular coordinates over time for the legs of the figure. Then, we use these pre-specified relative angular motions as constraints in a dynamic simulator which handles automatic collision detection and response. During the simulation, the body copes with both unknown internal forces at hinges (due to constrained motion) and external forces such as gravity and interactions with the ground. Solving for the constraints gives us the internal actuator forces over time.

---

[†]iMAGIS is a joint project of CNRS, INRIA, Institut National Polytechnique de Grenoble and Université Joseph Fourier.

The remainder of this paper develops as follows: Section 2 reviews the informations on human walking given by biomechanics and deals with their conversion into the constrained motion of an articulated human figure. Section 3 describes the simulator we will use for internal forces computation, i.e., the way we combine collision processing with forward and inverse dynamics. Our results on the dynamic analysis of a standard walk are presented in Section 4. Analysis and validation of these results is provided in Section 5. Section 6 concludes by discussing applications and work in progress.

## 2    The kinematics of human walking

This section reviews results on human walking described by biomechanics, and explains how we have converted them into parametrized automata generating different walking gaits for a human figure.
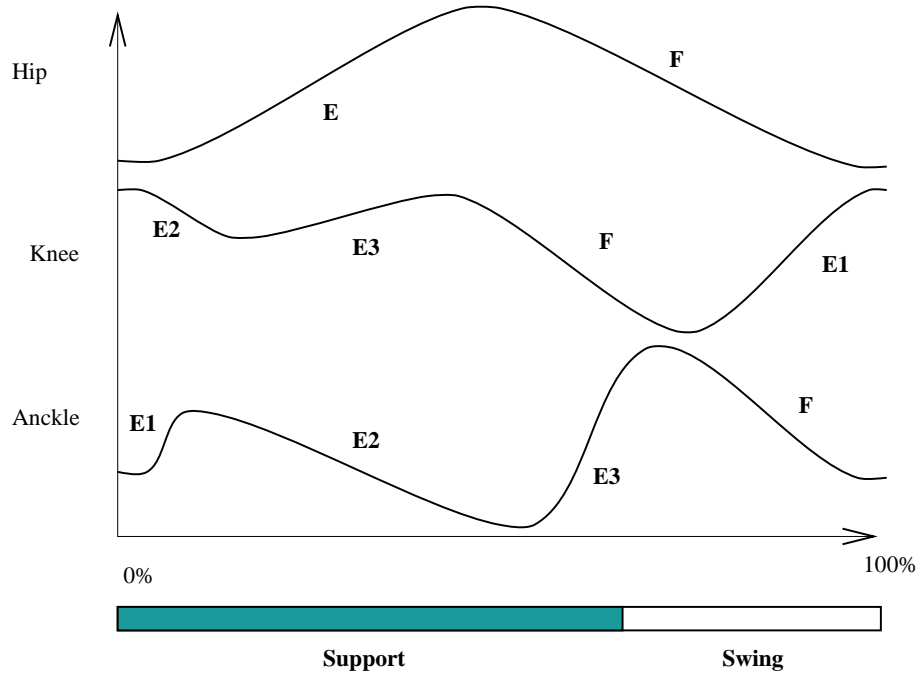
### 2.1    Biomechanical analysis of human walking



Figure 1: Angular laws of the limbs and locomotion sub-cycles during human walking.

A lot of studies on human walking can be found in bio-mechanics papers. Most of them characterize the different phases that compose the locomotion cycles. A more accurate description of these phases is provided by Nilsson [NTH85]. In particular, he identifies changes in angle trajectories between the different limbs of the legs depending on the velocity of the subject. Contrary to the other studies, he gives a locomotion sub-cycle for each articulation, by introducing phases of extensions/flexions. Each phase is defined by its position in the walking cycle, its duration, and the associated lower and upper angle bound values. In the example of figure 1, three phases during the extension of the leg are identified for the knee ($E_1$, $E_2$, $E_3$). One phase during flexion of the leg ($F$) completes the walking cycle.

The coordination between the articulations is given by the position and duration of the sub-cycles in the entire locomotion cycle. Nilsson analyses the effects of the variations of the velocity of the walk on these coordination parameters. In practice, we use linear laws for modeling these changes.

The velocity $V_G$ of a walker depends on the step length $L_{Step}$ and frequency $F_{Step}$ : $V_G = L_{Step} * F_{Step}$. So, for a given velocity, many possible step lengths and frequencies are possible. Enoka [Eno94] shows that people prefer, to a certain extend, increase their velocity by increasing $L_{Step}$ instead of $F_{Step}$. Nevertheless it is possible to customize a walking gait by tuning this strategy.

## 2.2   Knowledge-based kinematic model

To perform dynamic analysis of human walking from the results above, we first have to convert them into a parametrized kinematic model of human walking (more details on this model can be found in [MA97]).

We use Hierarchical Concurrent State Machines (HCSM) to model the locomotion sub-cycles described by Nilsson, and to ensure coordination between the articulations. The main state machine describes the global walking cycles : each state corresponds to a specific global sub-cycle such as stance phase, swing phase, double stand, etc. *Children* parallel state machines describe the sub-cycles local to each articulation. Linear laws are used to define how these sub-cycles change depending on velocity. Thus, if a change of velocity occurs, all the states are synchronized using the new sub-cycle parameters.

Each sub-cycle is described by its dates of activation and end, and the angular values of the articulation at these times. Intermediate values are interpolated. Since the forces we are going to compute are second order derivatives of motion, a very smooth interpolation is required. We thus set to zero first and second order derivatives at the bound values and use a polynomial of degree 5 in each interval (see figure 2). This ensures that the sign of angular velocity remains constant during the sub-cycle (positive for an extension, negative for a flexion), and leads to a smooth angular motion with $C^2$ continuity.
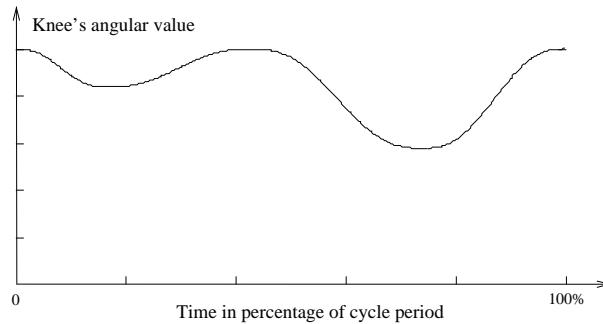


Figure 2: Approximation of the knee angle trajectory by 5-degree polynomial.

To customize the model and enable different walking gaits, we use tunable parameters for step length, step frequency and step height. Changing the step frequency simply corresponds to a change in the duration of the whole cycle whereas changing step length or height corresponds to a modification of the angular values of all the local states. This produces different walking gaits that will be analyzed in Sections 4 and 5 together with the standard gait described by Nilsson.

# 3   A simulator handling collisions and constrained motions

Combining the use of forward and inverse dynamics is a well known approach [IC88] but has not been applied, to the authors knowledge, to human walk including automatic collision detection and response along with a precise computation of closed loop forces and friction. Among related previous works, Boulic [BM94] performs static analyses of human postures. Ko and Badler [KB97] use an *ad hoc* inverse dynamics algorithm to modify human gaits according to force constraints, with approximate closed-loop force computation and a simplified contact model. Comparing our work with their results is not easy, since they do not provide curves of actuator forces during a walking cycle. However, our method makes no simplification for the contact (a linear displacement of the contact point on the foot was assumed by Ko and Badler), fully considering collision and friction, and handles with no simplification the calculus of torques when closed loops appear.

In order to perform a precise computation of the forces involved in a given walking gait, we use a general simulation algorithm, designed to handle arbitrarily large scenes with contact and friction. Applied to a human figure, it allows the computation of very general interactions between the figure and the universe. These interactions include frictioning contacts such as contact with the ground

and collisions with arbitrary moving or stationary obstacles. Other applications of this general interaction processing include object grasping, and synchronization between several human figures (such as walking hand in hand).

## 3.1 Accurate closed-loop force computation

Our simulation algorithm relies on absolute coordinates for purpose of generality. A joint is represented by a set of geometric constraints on the relative motions of the bodies at the center of the joint. Each of them constrains the relative motion of the bodies along a given direction (thus, vectorial constraints are turned into sets of scalar constraints). For example, a standard revolute joint involves five scalar constraints: three orthogonal null translation constraints and two orthogonal null rotation constraints along directions orthogonal to the axis of the joint.

During the simulation, the algorithm computes the Lagrange multipliers of the constraints, i.e., scalar independent forces (or torques) associated with each independent scalar constraint. This is done in three steps:

1. we first compute the influence of inertias or external forces on the bodies by animating them while assuming null constraint forces;

2. then, we compute the constraint errors by projecting the relative motions (accelerations, velocities or linearized displacements) in the direction of each scalar constraint;

3. finally, we reach a global solution by finding the constraint forces necessary to cancel the constraint errors.

For the third step, Baraff [Bar96] recently presented an algorithm that works in linear time on acyclic structures in absolute coordinates. An additional dense matrix solution is used for handling closed-loop constraints. We use the same linear-time solution to solve the acyclic constraints. However, since our simulator is designed for handling arbitrarily large scenes, we wish to avoid any dense matrix solution. We prefer to handle closed-loops by progressively refining a global solution, thanks to an iterative conjugate gradient-based minimization of the closed-loop constraints. It uses a Fletcher-Reeves-Polak-Ribiere method [PTVF92] to compute the closed-loop forces necessary to enforce the closed-loop constraints. This allows the time complexity to smoothly range from linear to quadratic in the number of constraints according to the number of closed-loop constraints, with a tunable precision of the computed forces.

## 3.2 Handling inverse dynamics in the simulation algorithm

In addition to fast forward dynamics, our simulator can be used to perform inverse dynamics (i.e., internal forces computation) on joints with pre-defined angular motions. We just have to take the desired pre-defined motion into account during the computation of the constraint errors (step 2 of the simulation algorithm above). Then, the Lagrange multipliers give us the internal forces which are necessary to meet the animation constraints.

For instance, a revolute joint with a driven rotation involves six independent constraints, including a (generally) non-null relative rotation constraint along the axis of the joint. The joint forces necessary to achieve the motion are thus computed without any change in the simulation algorithm.

## 3.3 Collisions, contacts and friction

We detect a sphere-plane collision when the distance between the center of the sphere and the plane is less than the radius of the sphere. The contact point is modeled by projecting the center of the sphere on the plane, and the relative velocity at the contact point is canceled using an impulsion.

We use a subclass of joints for modeling contacts. A contact joint is characterized by a constraint on the motion along the normal of the surfaces in contact at the contact point. This allows us to take the contact into account in the global force computation algorithm.

| Part | Mass (% of total weight) | Length (% of total height) |
|------|--------------------------|----------------------------|
| Head | 7.84 | 10.0 |
| Trunk | 53.13 | 28.7 |
| Upper Arm | 2.96 | 18.8 |
| Lower Arm | 2.20 | 14.5 |
| Upper Leg | 7.92 | 24.5 |
| Lower Leg | 4.70 | 24.6 |
| Foot | 1.72 | 8.9 |

Table 1: Measurements of the mass and size of the different body parts.

The Coulomb constraints on contact forces and motions are handled using an iterative global solution algorithm [Fau96]. The latter was initially designed for dense matrix dynamics solution, but we adapted it to the sparse matrix formulation. A contact joint is destroyed when the force necessary to enforce the motion constraint corresponds to an attraction instead of a repulsion between the two solids. Then, a new force computation is performed.

# 4    Inverse dynamics applied to human walking

## 4.1    Simulating a standard gait of a human figure

The human figure model that we use is built of rigid links connected by rotational joints. Since we only have a 2D information on the walking motions (see Section 2), using joints with a single rotational degree of freedom is sufficient. The masses and sizes of the different limbs, given in table 4.1, are those of a male human adult. For each limb, the associated mass matrix is computed assuming a uniform density and a cylindrical shape of the limb.

The standard walking gait depicted in Figure 3 was generated using the angular laws described in Section 2, which define driven angular motions for the articulations of the legs. The cycle period, i.e., the interval between two consecutive stands of the same foot is one second, which corresponds to a slow walk. For the arms, we chose articular laws which gave a natural neutral swing. To position the body completely, we enforce a constant angle between the trunk and the ground. During the simulation, the human figure copes with gravity, collisions and Coulomb friction with the ground, simulated by a sphere-plan contact (see Section 3), so the driven motion of the legs makes the body move forwards.
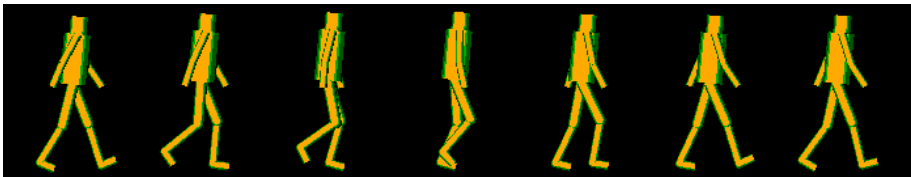


Figure 3: Snapshots of the motion, during a step. We define a step by the interval between two consecutive stands, the cycle is made of two steps.

The simulation was achieved in interactive time(2.5 frames per second) on a SGI Indigo2 Workstation. Our aim is now to analyse the torques produced at the leg joints during one cycle of this walking gait.

## 4.2    Actuator torque curves during one step

Computations have been performed by applying our reference gait with the inverse dynamics algorithm described in Section 3.2. Played on the video, the result is an irregular gait. The character stops and starts again at each step. This is due to the difference between our angular laws and those of a real human gait. Figure 4 plots the values of the torques for the hip, the knee, and the ankle during one cycle period. We noticed that our method has a good numerical stability, as the

shape of the resulting plots converged to a solution when we increased the sampling rate. Results are shown with a simulation sampling rate of 30Hz.
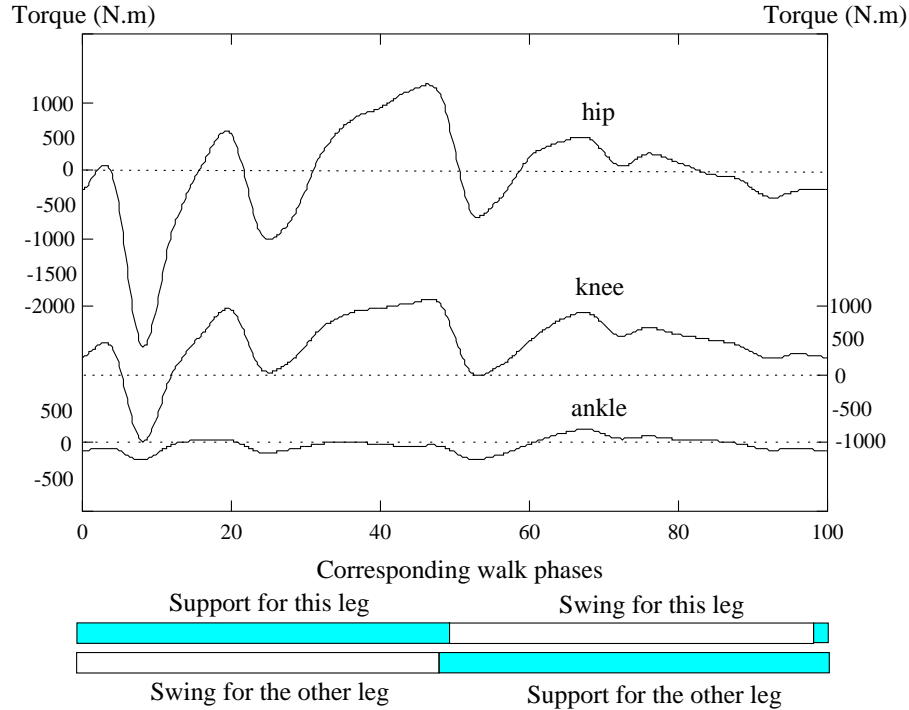


Figure 4: Computed torques for the hip, the knee and the ankle of a leg during a step. For each plot, a new zero axis is drawn, all measured in percentage of the cycle period, the scales on the ordinate are the same for the three plots, measured in $N.m$.

All the torques we computed with this gait are rather continuous, have a one second period, and only slight differences appear between two periods. The torques measured at the hip are greater than those of the knee, but their shape look alike. The torques of the ankle have lower values. This gives the first qualitative validation of our results.

We first notice the high values of the computed torques. This can be explained by the irregularity of the gait. The character stops and starts again twice a period. The total period is one second. If we approximate the velocity using lines segments, an average velocity of 1.5 $m.s^{-1}$ requires an average acceleration of $\pm 6$ $m.s^{-2}$. Since the mass of the character is 80 $kg$ and the distance between its center of mass and the ground is 1.2 $m$, this implies a $\pm 576$ $N.m$ average torque. This is a first numerical confirmation of the visually noticeable shortcomings of the gait. Another dynamic result confirming these problems is the fact that we could not prevent the character from sliding, even with a friction coefficient as high as 1.

Interpreting the evolution of the torques according to the events appearing during walking is also important. The support phase is characterized by a negative propulsive torque, which corresponds to an acceleration of the character, followed by a positive torque, corresponding to the deceleration. The swing phase generates a lower positive torque that brings back the leg.

## 4.3  Biomechanical validation

Biomechanics researchers [Ped77, BLA94] have measured the interaction forces between the feet and the floor when a real subject walks. Their results are depicted in Figure 5(a).

A way to validate our computations is to compare our own results with these curves. Figure 5(b) give the vertical interaction force with the floor during our simulated walk, as ploted by our simulator. Bouncing occurs when the foot hits the ground, due to numerical instabilities. Except for the artifact due to the unwanted flying phase generated by our simulation, the curves are quite similar.
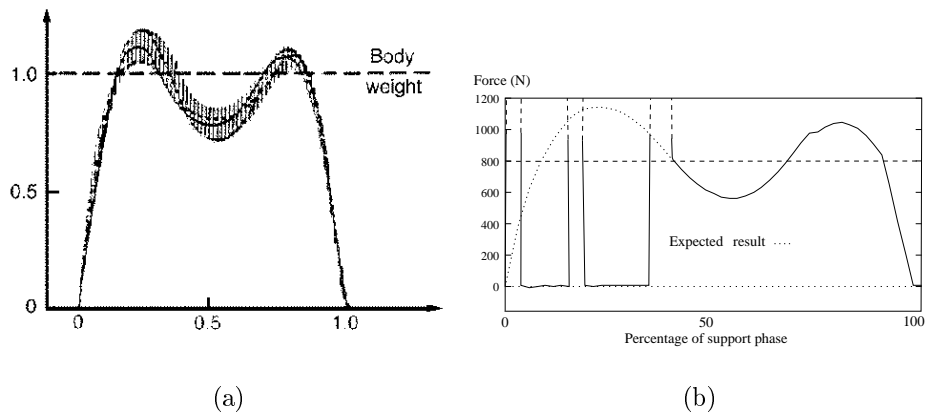
Figure 5: Action on the ground during the support phase. Measured (a) and computed (b) exhibit similarities. Our character mass was 80kg.

## 4.4   Influence of body mass

We changed the parameters of our character and measured the evolution of the torques. A modification of the total weight of the character, while keeping the mass repartition, changes the amplitudes of the torques in a scale close to the scale of the change of weight. The global shape remains the same. See Figure 6. Notice that this change of mass slightly changes the computed torques during the swing phase, when the leg does not support the body.
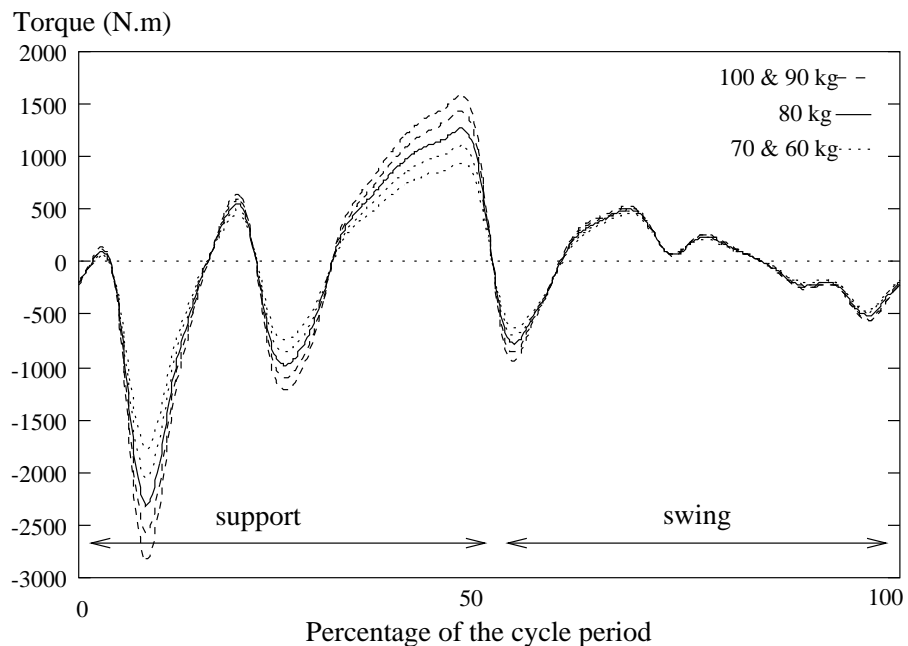


Figure 6: Influence of the mass of the human figure on the hip torques.

**Comparison of different walking gaits**

We know study the influence of the gait on our computations. We compare four different gaits including the standard one we previously studied. The three new gaits are: one with long steps (1 second period), one with short steps (0.62s period) and a walk with "goose" steps (0.82s period).

The results are plotted on Figure 7 after appropriate time scaling. As one can see, the global shape remains the same, with differences in the values. The short step gait involves the lowest torque values. On video, it is also the gait generating the most regular velocity of the character and thus,
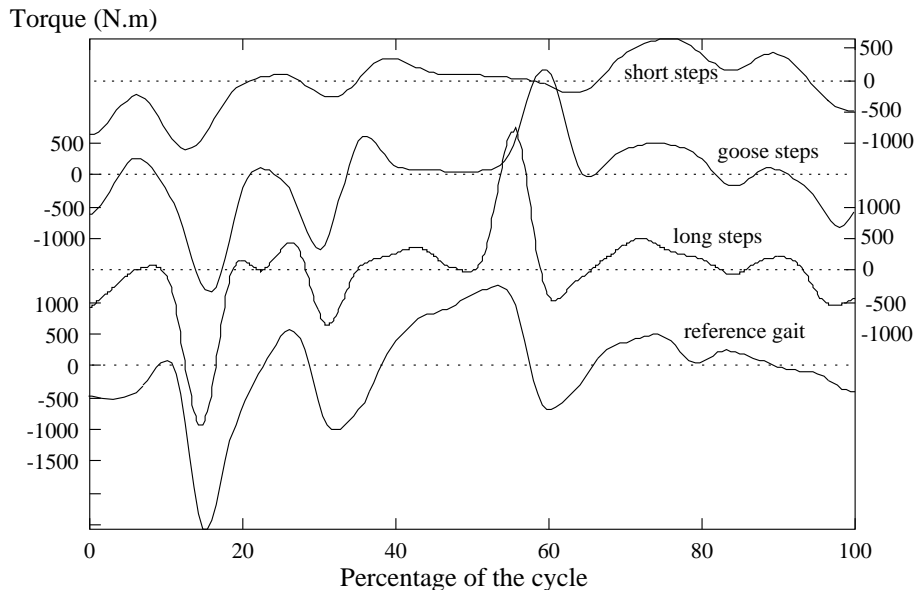
Figure 7: Comparison of the different gaits, here shown with the computed torque for the knee.

the most realistic among the four gaits.

# 5 Applications and concluding remarks

This paper has presented an analysis of the torques produced in the legs of a human figure during walking. Our computations are based on a kinematic description of walking gaits given by biomechanics, and on a robust simulator that combines forward and inverse dynamics and handles collisions and friction between the figure and the floor. Visually noticeable motion shortcomings could be confirmed by unexpected numerical values. The most visually plausible gait corresponds to the most plausible articular torques.

The results we give can be exploited in two different applications:

- They provide data to researchers in biomechanics who can analyse, for instance, the way a human combines the use of its different muscles in various walking gaits.

- They can help the design of realistic controllers dedicated to walking motions, and thus be used in a physically-based simulation of walking.

In addition, our simulator which delivers the torques during pre-specified motions, could be used in cooperation with a purely kinematic animation system, for warning the user when the motion is unfeasible (i.e., when torques exceed a given threshold).

Although sufficient for performing an initial analysis of the dynamics of human walking, our results have been altered by different artifacts. First, we did not have any captured motion to start with. The kinematic data we injected into our simulator were not very accurate, although derived from biomechanical descriptions. In particular, the variations of the angle between the body of the human figure and the world coordinate system were missing. Our choice of a constant angle (see Section 4) was not very realistic. Performing the same computation on real walking data, with 3D instead of 2D trajectories, would undoubtfully give more accurate results. Moreover, our use of rigid body collisions for simulating the interactions between the feet and the ground was not very satisfactory, since it resulted in short unwanted flying phases, during which torques could not be accurately evaluated. We are currently adding "soft shoes" to our human figure in order to avoid these extra flying phases and hopefully get better results. A better starting motion is also expected to reduce this bouncing phenomenon.

# References

[Bar96]     David Baraff. Linear-time dynamics using lagrange multipliers. In *SIGGRAPH 96 Conference Proceedings*, Computer Graphics Proceedings, Annual Conference Series, pages 137–146. ACM SIGGRAPH, Addison Wesley, August 1996. ISBN 0-201-94800-1.

[BC89]      A. Bruderlin and T. Calvert. Goal-directed, dynamic animation of human walking. *Computer Graphics*, 23(3):233–242, July 1989.

[BC93]      Armin Bruderlin and Tom Calvert. Interactive animation of personalized human locomotion. In *Proceedings of Graphics Interface '93*, pages 17–23, Toronto, Ontario, Canada, May 1993. Canadian Information Processing Society.

[BLA94]     F. Barbier, P. Loslever, and J-C. Angue. Méthode informatisée de mesure et d'analyse des forces de réaction et des angles articulaires de la marche normale. *Innov. Tech. Biol. Med.*, 15(4):453–460, 1994.

[BM94]      Ronan Boulic and Ramon Mas. Inverse kinetics for center of mass position control and posture optimization. Technical report, Ecole Polytechnique Fédérale de Lausanne, September 1994.

[BW95]      Armin Bruderlin and Lance Williams. Motion signal processing. *Computer Graphics*, August 1995. Proceedings of SIGGRAPH'95.

[Eno94]     R. M. Enoka. *Neuromechanical Basis of Kinesiology (2nd Edition)*. Human Kinetics, 1994.

[Fau96]     François Faure. An energy-based method for contact force computation. *Computer Graphics Forum*, 15(3):357–366, August 1996. (Proceedings of EUROGRAPHICS'96).

[HWBO95]    Jessica Hodgins, Wayne Wooten, David Brogan, and James O'Brien. Animating human athletics. *Computer Graphics*, August 1995. Proceedings of SIGGRAPH'95.

[IC88]      P.M. Isaacs and M.F. Cohen. Mixed method for complex kinematic constraints in dynamic figure animation. *The Visual Computer*, 2(4):296–305, December 1988.

[KB97]      Hyeongseok Ko and Norman Badler. Animating human locomotion with inverse dynamics. *IEEE Computer Graphics and Applications*, March 1997.

[LvdP96]    Alexis Lamouret and Michel van de Panne. Motion synthesis by example. In *Computer animation and Simulation'96*, pages 199–212. Eurograpics workshop, September 1996.

[LvdPF96]   Joseph Laszlo, Michiel van de Panne, and Eugene Fiume. Limit cycle control and its application to balancing and walking. *Computer Graphics*, August 1996. Proceedings of SIGGRAPH'96.

[MA97]      F. Multon and B. Arnaldi. A biomechanical model for interactive animation of human locomotion. Submitted to the Journal of Visualization and Comp uter Animation, March 1997.

[NM93]      J.T Ngo and J. Marks. Spacetime constraints revisited. *Computer Graphics*, August 1993. Proceedings of SIGGRAPH'93 (Anaheim, California, August 1993).

[NTH85]     J. Nilsson, A. Thorstensson, and J. Halbertsam. Changes in leg movements and muscle activity with speed of locomotion and mode of progression in humans. *Acta Physiol Scand*, pages 457–475, 1985.

[Ped77]     A. Pedotti. A study of motor coordination and neuromuscular activities in human locomotion. *Biological Cybernetics*, pages 53–62, 1977.

[PTVF92]    Press, Teukolski, Vetterling, and Flannery. *Numerical Recipes in C*. Cambridge University Press, 1992.

[RGBC96]    Charles Rose, Brian Guenter, Bobby Bodenheimer, and Michael Cohen. Efficient generation of motion transitions using space-time constraints. *Computer Graphics*, August 1996. Proceedings of SIGGRAPH'96.

[UAT95]     Munetoshi Unuma, Ken Anjyo, and Ryozo Takeuchi. Fourier principles for emotion-based human figure animation. *Computer Graphics*, August 1995. Proceedings of SIGGRAPH'95.

[vdPF93]    M. van de Panne and E. Fiume. Sensor-actuator networks. *Computer Graphics*, August 1993. Proceedings of SIGGRAPH'93 (Anaheim, California, August 1993).

[WP95]      Andrew Witkin and Zoran Popovi'c. Motion warping. *Computer Graphics*, August 1995. Proceedings of SIGGRAPH'95.